An Improved Framework for Hybrid Energy Harvesting for Underwater Sensor Nodes and IoT

GAURANG GUPTA
Netaji Subhas University of Technology

Abstract- ***Energy harvesting for sensor networks deployed at critical locations is an important research area now these days. Various types of energy harvesting techniques like solar, thermal, aquatic, wind energy harvesting systems are very popular in research community. This is found in the survey, that single energy harvesting technique is not enough for the wireless sensor network, specially when the nodes are deployed at critical areas like volcanoes, underwater, ocean, rivers etc. Finding energy solutions for perpetual, batteryless, and critical places where human intervention is not possible is the motivation of this paper. In this paper, a hybrid energy harvesting solution using solar, pressure, and thermal has been proposed. An optimized framework has been proposed, implemented, and analyzed for underwater sensor network application. A mechanical and an electrical schematic has been designed, implemented, and realized. The physical parameters of solar, thermal, and piezoelectrical transducers has been analyzed along with mathematical equations to find the best possible solutions for the optimized framework. The model is theoretically implemented and investigated, and this is found that 13.66KJ of energy can be extracted in 24Hrs from the proposed design which guarantees a perpetual lifetime of sensor node.***

Indexed Terms- ***Energy harvesting, Sensor network, underwater sensor network, Solar, thermal, piezoelectric.***

I. INTRODUCTION

Sensor technologies have revolutionized, and we have advanced enough to deploy sensor technologies in different kinds of remote environments. More than 3/4th of the earth's total surface is covered with water (majorly rivers, oceans and seas) and it has become a necessity to monitor these environments to get informative and utilizable data [1]. With the development of new technologies, we have new ways to sense marine environments [2,3]. There are a wide range of applications [4-12] of underwater sensing such as water quality monitoring, recording the quantity of pollutants and toxins, marine surveillance, aquaculture, climate recording, prediction of natural disasters, study and survey of marine environments and other commercial applications such as oil industries etc.

Along with the several problems in deploying sensor nodes underwater one major problem is the energy needs of the sensors [13]. Since, these sensors are deployed in remote areas underwater which might not be easily accessible, it is very difficult to maintain and replace batteries of these sensor nodes. Depleted batteries would then interfere with the proper functioning of the sensors and would compromise with its performance [14-19].

Hence, we come up with a hybrid model of harvesting energy easily and efficiently which would require very little maintenance. These harvesting techniques would replace the batteries, be pollution free and harmless to aquatic life [20, 21]. They would not compromise with the performance of the sensors and networks as they are inexhaustible. We are converting waste physical energy in the environment into usable electrical energy [22]. Relying on one source of energy wouldn't be wise as it may be possible that it's not available at some point of time [23]. Hence, we came up with a model that utilizes three different sources of energy as one might not be enough to satisfy the energy needs of the sensor node for a perpetual lifetime [24].

We propose to utilize solar, thermal energies and piezoelectricity in the same hybrid model. Solar energy can be easily generated using PV (Photovoltaic) cells. However, it is not possible to harness solar energy during night-time. For that purpose, we have a thermal electric generator (TEG) installed in our model. Harnessing piezoelectricity from the mechanical stress applied by water molecules would ensure a continuous supply of power to the sensor nodes as it would be always available in the oceans/seas.

Further, the paper is configured as follows. Section I contains the introduction of the energy harvesting techniques; Section II is associated with literature review and related work. Section III, is related to proposed framework of hybrid energy harvesting modules. Section IV, shows the parameters related to solar, thermal and piezoelectric energy transducers. Section V having the simulation and results. And finally, conclusion of the paper has been drawn in section VI.

II. RELATED WORK

According to [25], the efficiency of Si cells can be improved by the technique of Multi Junction Solar Cells . These cells contain more than one layer of PV cells with many different energy band gaps attached together and this results in a better usage of the solar spectrum.

In [26], the researchers have turned a wearable jacket to an energy harvesting system. It was observed that the system harvested 0.9mW of energy during sitting posture. This technology had 16 PV Cells, 12TEGs and 5 power management Integrated Circuits (ICs). This model is capable of powering 2 AAA NiMH batteries in series. The solar and thermal harvesting chips used were TI BQ25504. By using a PV Cell on top of a TEG the authors observed a 4-5% gain in efficiency.

In [27], the authors came up with the idea of using a DC-DC boost converter in a thermal energy harvester, which produced usable electrical energy from waste thermal energy. This thermal energy was used to power Wireless Sensor Nodes(WSN) to improve their working lifetime.

In [28], a macro level thermal energy harvesting technique was proposed which was inexpensive but the temperature difference between both sides created a major issue. A minimum of 10OC of temperature difference must be there between both sides of the TEG for an efficiently working system.

Authors in [29], proposed a TEG model to harvest thermal energy that generated several joules of energy. It was suggested that better heat sinks and larger supercapacitors would solve the problem of the less temperature difference between 2 sides of the TEG. In [30], a simulated model was presented which controlled the DC-DC converter duty cycle to obtain maximum TEG Power.

In [31], a system to supply power to low power sensors in aircrafts using TEG was presented. In which TEG's open circuit voltage is measured automatically as part of a power management technique and the maximum harvested power is recorded. In [16], Alper and Ghislain experimentally investigated and proved the concept of piezo hydroelasticity for underwater thrust and power generation, they found out that The average power requirement for generating a mean thrust of 19 mN at 6 Hz is measured as 120 mW. A 50.8mm×25.4mm×0.017 mm thin film battery (2.5 mAh, 4 V) can provide this power for 5 min.

In [14], the authors examined different power management schemes and energy harvesters with an objective of underwater node lifetime improvement. The authors used ambient energy present in water flow and acoustic waves and converted them to electrical energy using hydrokinetic turbine, piezoelectric cantilever, and hydrophone to supply power to nodes.

III. PROPOSED FRAMEWORK

To run the Underwater Sensor Network (UWSN) nodes continuously, we have used techniques to harvest power from inexhaustible resources. Three sources of energy in a single system to make it reliable and efficient has been used. Solar cells are placed to harvest solar energy at the topmost layer of our hybrid model, it is followed by an Aluminum Plate and a water chamber. At the bottom, a Lead Zirconate Titanate (PZT) crystal which harvests piezoelectricity has been used. The whole model will be placed on a buoy to keep it over the water surface with just PZT crystal exposed to the water. An electrical schematic has been also with passive components to channelize the stored energy in proper way. Following are in detail discussion about the mechanical and electrical schematic.

a. Mechanical Schematic

Figure 1 shows the mechanical schematic. The topmost layer, i.e., Photovoltaic (PV) Cells collect photons from the sunlight and subsequently convert it

into electrical energy. An Aluminum plate is placed just below the solar cells. Aluminum is a great conductor of heat, so it gets heated in the daytime. Beneath that is a Thermoelectric Generator (TEG) which works on peltier's effect and convert the gradient of thermal energy into electrical energy. A chamber which contains the Phase Change Material (PCM) i.e. water is present beneath the TEG. After that a PZT crystal which is exposed to water is present, this PZT crystal generates Piezoelectricity, converting the mechanical stress generated by water molecules into usable electricity. This is the last layer of proposed mechanical schematic model.

Phase change material (PCM) is a material used in thermal electric generators which store/dissipate energy whenever there is a change in phase, for eg: gaseous to liquid. This heat is absorbed and stored and can be used after some time. During the day, water (PCM) is cooler than the Aluminum plate and heat flows from Al to Water and the TEG generates electricity utilising this flow of heat. The opposite happens during the nighttime when the Al plate is cooler than water and there is heat flow from Water to Al, the TEG utilizes this flow of heat as well and generates usable electricity. The PZT crystal experiences stress from the water molecules beneath it, this stress polarizes the ferroelectric crystal and generates utilizable electricity.

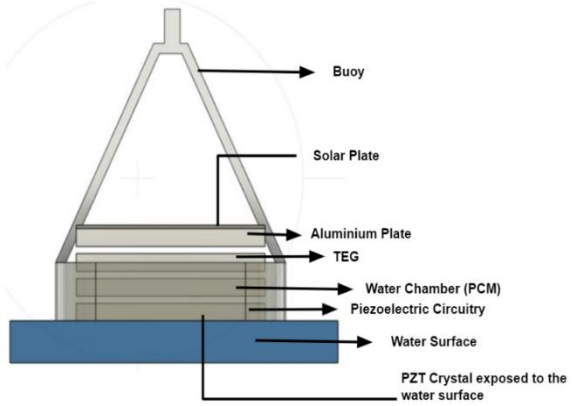

Figure 1: Mechanical Schematic

The buoy keeps the arrangement on the surface of water preventing it from sinking. It has been created such that there is access to air for the water chamber. The solar plate generates solar energy. The Al plate and water chamber are important for the functioning of the TEG. Below that is the required circuitry needed to harness piezoelectricity (which will be discussed in the later sections). The PZT crystal is placed beneath this arrangement.

b. Electrical Schematic

The electrical schematic as proposed is given in figure 2. The given circuit shows the implementation of our model electrically. We use a buck-boost converter IC i.e REES52 to convert the voltage to 5.5V to charge the capacitor. Between the output of the buck-boost converter and the capacitor is a MOSFET acting as a switch. This switch will be closed until the capacitor has 4.86V or less than that; as soon as it has a greater voltage than 4.86V the switch will open and prevent overcharging or overflow of current. This voltage comparison is done using an Op-Amp LM311.

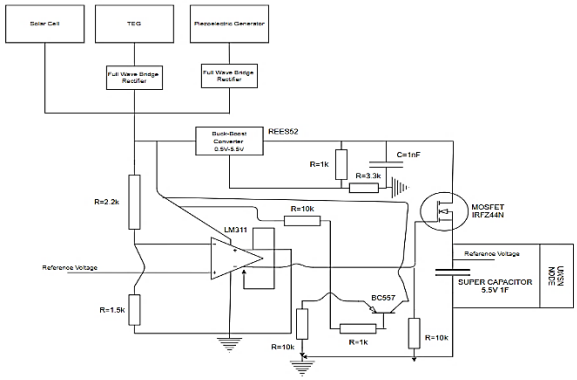

Figure-2: Electrical Schematic (All values of resistances are in Ω)

A full wave bridge rectifier has been used with the TEG to ensure supply of current in a single direction. A voltage divider circuit has been used with the output of the converter to regulate the voltage exactly at 5.5V. We have used an LM311 comparator IC to compare the voltage values of the supercapacitor and the input voltage. This input voltage is supplied to pin number 2 of the op-amp using a voltage divider circuit. The resistors 2.2k and 1.5k drop a voltage of 4.86V from the input. This 4.86 volt is compared with ref voltage (voltage of capacitor) which is connected to pin 3. When the ref voltage is smaller than 4.86V the output pin 7 will go high and the input voltage with the pull-up 10k resistor. This voltage will then be used to operate the MOSFET. The IRFZ44N MOSFET is used to connect the super capacitor and the charging voltage which is manipulated by the signal from the op-amp. When the op-amp goes high it supplies the input voltage on pin 7 which turns on the MOSFET through

its base pin. The same happens when the op-amp goes low (0V), the MOSFET will be opened. We also have a PNP transistor BC557 which prevents the extra flow of current reducing the wastage and loss of power in the circuit.

The capacitor is connected directly to the UWSN node, this node draws voltage from the capacitor as per its needs and the sensor runs continuously without any issue. Neither the performance nor the efficiency of the sensor is compromised.

IV. PARAMETERS

Parameters of TEG, PV cell and PZT has been discussed in this section. Parameters may help us to design the optimal solution of the hybrid energy harvesting. The details of parameters are as follows:

a. TEG Parameters

The parameters which affect the working of TEGs are Seebeck Coefficient (greater the value of Seebeck Coefficient greater is the conversion of thermal energy to electrical energy), thermal conductivity (measure of a material's ability to conduct heat), load and internal resistances and heat transfer. Table 1 shows the parameters of Bismuth Telluride (Be_2Te_3). More details of the parameters have been considered from [28]. Readers may follow the [28] for more details

Table 1: Values of Parameters of TEG for Be_2Te_3

S.No.	Parameter	Notation	Value
1.	Thermal conductivity of Ceramic Substrate	λ_{Sub}	180W/mK
2.	Thermal conductivity of Thermocouple	λ	1.5W/mK
3.	Substrate Thickness	L_{Sub}	0.9mm
4.	Antimony Telluride (p-type) Seebeck Coefficient	α_p	185μV/^{o}K
5.	Bismuth Telluride (p-type) Seebeck Coefficient	α_n	-228μV/^{o}K
6.	Electrical conductivity of n-type	ρ_n	12.6$\mu\Omega$m
7.	Electrical conductivity of p-type	ρ_p	12.6$\mu\Omega$m
8.	Length of thermal element	L	1.6mm
9.	Total number of thermocouples	N	127
10.	Thermal conductivity of n-type	σ_n	1.8W/mK
11.	Thermal conductivity of p-type	σ_p	1.3W/mK

Figure of merit of TEG is directly proportional to the square of the Seebeck Coefficient. The material's ability to generate Thermal Energy is dependent on the figure of merit. Hence for a high conversion rate of thermal energy to electrical energy, a high value of Figure of merit (ZT) is needed. Eq. 1 below gives the value of ZT

$$ZT = \left(\frac{(\alpha n-\alpha p)^2}{\sqrt{\rho n\,\sigma n}+\sqrt{\rho p\,\sigma p}}\right)T \quad (1)$$

Here T is the average temperature of the TEG module. The eq. 2 below gives the efficiency of the TEG-

$$\eta_{TEG} = \frac{\Delta T(\sqrt{1+ZT}-1)}{Th(\sqrt{1+ZT}+\frac{Tc}{Th})} \quad (2)$$

The efficiency of the TEG Module is directly proportional to the temperature difference $\Delta T$and ZT.

b. Solar Cells Parameters

Photovoltaic (PV) Cells called solar cells harvest electrical energy from solar energy. Photons from the sun strike the semiconductor layer of the solar cells and generate electron-hole pairs; these free electrons then flow in the external circuit as electric current.

Solar panels, which are a combination of many solar cells, are used as they generate a higher voltage. Each Si solar cell can produce around 0.5-0.6volts. Following are the equations in support of PV cells.

$I= N_pI_{ph} -I_d -I_{Rsh}$ (3)

$I_{ph}=[I_{sc} + k_i(T- T_{ref})]\frac{G}{Gref}$ (4)

$I_D=I_S[\exp(\frac{qVd}{nKT} - 1)]= I_S[\exp(\frac{q(V+IRs)}{nNsCKT} - 1)]N_P$ (5)

$I_S=I_{rs}(\frac{T}{Tn})^3\ exp[\frac{qEgo(1/Tn - 1/T)}{nK}]$ (6)

$I_{sh}=(\frac{V + IRs}{Rsh})$ (7)

$V_T= \frac{KTop}{q}$ (8)

$V_{OC}=V_t ln(\frac{Iph}{Is})$ (9)

$\eta = \frac{Voc\ Isc\ FF}{Pin}= \frac{Vmpp\ Impp}{Pin}$ (10)

$FF=\frac{Max\ Power}{Voc\ Isc}$ (11)

c. PCM (Phase Change Material)

PCM is a material that stores energy when there is a change in state at the Phase Change Temperature (PCT), this stored energy is later radiated and utilized efficiently. For the efficient performance of the TEG, the PCM plays an important role hence it must be chosen very carefully. Here we choose water as the suitable PCM because it has high volumetric latent heat storage capacity and it is easily available at a low cost., It has sharp melting point, high thermal conductivity, high heat of fusion of approximately 333.6kJ/kg, non-flammable, chemical stability, completely reversible freeze/melt cycle, no degradation after many freeze/melts cycle, non-corrosiveness, non-toxic and non-explosive material. Apart from this it also has a high energy of phase change, high latent heat, and high specific heat. Higher thermal conductivity leads to a greater ease of transfer of heat from the TEG module. The TEG's operating temperature conditions are also satisfied if water is used as the PCM.

d. Piezoelectric Generator

The Piezoelectric generator harvests energy by converting the mechanical stress/vibrations to usable electrical energy. The performance and the conversion rate depend on the piezoelectric material used and many other factors discussed below-

Density, piezoelectric coefficients, relative permittivity, electromechanical coupling factor and mechanical quality factor. We're using PZT-5H which is DOD Type VI, Lead-Zirconate Titanate it has the following properties -Very high strain (charge) constants, permittivity, and coupling constants, Modest Curie temperature restricts its temperature range and thermal stability, low mechanical quality factor, high charge output useful for sensing devices and generator elements, high strain output useful for large displacements at lower voltages, used for sensing (receivers, knock, hydrophones, pick-ups, medical diagnostics), used for actuators (valves, positioning, fans, tilters). The values of the various parameters have been given below for PZT-5H

Piezoelectric coefficients(d) in pC/N : d_{15}=741, d_{31}=-274, d_{33}=593; Relative Permittivity (ε_r) :ε_{11}=3130, ε_{33}=3400; Electromechanical Coupling factor (k): k_{15}=0.68, k_{31}=0.39, k_{33}=0.75; Quality factor=65; Density=7600 kg/m^3. PZT-5H has a high Curie Temperature hence providing a high thermal stability, The crystal structure of a material changes at the Curie temperature from piezoelectric (non-symmetrical) to a non-piezoelectric (symmetrical) form, and the material loses its piezoelectric properties. This phase change is accompanied by a peak in the dielectric constant at that temperature. The Curie temperature, Tc, is expressed in degrees Celsius. For PZT-5H T_C is 120°C which can be further increased by adding silver to the ceramic crystal. The piezoelectric coefficients (d_{33}, d_{31}, d_{15} etc.) measure the strain which has been induced by an exerted voltage (in meters per volt). High values of dij coefficients show larger displacements which are desperately needed for motoring transducer devices. The coefficient d33 measures deformation in the same direction (polarization axis) as the induced potential, whereas d_{31} describes the response when the force is applied perpendicularly to the polarization axis. The d_{15} coefficient measures the response when the applied mechanical stress is because of shear deformation. Relative permittivity (εr) is the ratio between the value of absolute permittivity of the piezoelectric material, ε, to the value of vacuum permittivity, ε0. The electromechanical coupling factor k tells us the effectiveness with which a piezoelectric material converts electrical energy into mechanical energy, or converts mechanical energy into electrical energy. The first subscript to k denotes the direction along which the electrodes are applied; the second denotes the

direction along which the mechanical energy is applied, or generated. The mechanical quality factor Qm is a major high-power attribute of piezoelectric ceramic materials. It is the inverse of the mechanical loss tan ϕ. Below is a table(3) which gives the values and meanings of all the notations used

Table-3: Notations used for Piezoelectric Generator with meanings and values

Notation	Meaning	Value for PZT-5H
K^T	Relative Dielectric Constant when there are no external forces	1700
k_{31}	Electromechanical Coupling Factor/Coefficient(applied stress is in 3 directions)	0.35
k_{33}	Electromechanical Coupling Factor/ Coefficient(applied stress around 2 axis)	0.69
T_C	Curie Temperature	120^OC
ρ	Density	$7600kg/m^3$
d_{31}	Piezoelectric Charge Coefficient(applied stress in 3 directions and electrodes along 1 axis)	1.8e-10 m/V
d_{33}	Piezoelectric Charge Coefficient(applied stress in 3 directions and electrodes perpendicular to 3 axes)	3.6e-10 m/V
g_{31}	Piezoelectric Voltage Coefficient(Applied stress in 1 direction and electrodes perpendicular to 3 axis)	0.011 Vm/N
g_{33}	Piezoelectric Voltage Coefficient(applied stress in 3 directions and electrodes perpendicular to 3 axes)	0.025 Vm/N
Y	Young's Modulus	63GPa
s	Compliance	$0.015X10^{-9}$ Pa^{-1}

The following equations (12) give us the formulae of all the parameters discussed above-

$$K^T=\frac{Co\ h}{\varepsilon o\ A} \quad (12)$$

Here K^T is the relative dielectric constant of the material, ε_o is the relative permittivity of free space($8.854 X 10^{-12}$ F/m), h is the distance between electrodes in metres, A is the area of electrodes in m^2 and C_o is the capacitance at 1kHz

$$Q_M=\frac{1}{2\pi\ Fr\ Zm\ Co}\left(\frac{Fa^2}{Fa^2\ Fr^2}\right) \quad (13)$$

Here F_r is the resonance frequency, F_a is the anti resonance frequency, Z_m is the impedance at F_r and C_o is static capacitance in Farad

$$k=\sqrt{\frac{Electrical\ energy\ stored}{Mechanical\ Energy\ Applied}}$$

$$\frac{kp^2}{1+kp^2}=\frac{(1-\sigma^E)J1\ [\eta1(1+\frac{\Delta F}{Fr})]-\eta1(1+\frac{\Delta F}{Fr})Jo[\eta1(1+\frac{\Delta F}{Fr})]}{(1+\sigma^E)\ J1\ [\eta1(1+\frac{\Delta F}{Fr})]} \quad (14)$$

Here k_p is the electromechanical coupling factor, J_o=Bessel function of the first kind and zero order, J_1= Bessel Function of the first kind and first order, σ^E is the Poisson's Ratio, η_1 is the lowest positive root of $(1+\sigma^E)J1\eta=\eta Jo(\eta)$

It has been assumed that for Lead Zirconate Titanate, $\sigma^E=0.31$and $\eta1=2.05$

And ΔF= F_a - F_r (Hz).

Defining one more parameter, x which is given as $x=\frac{\Delta F}{Fr}$

$$k_{33}^2=\frac{\frac{\pi}{2}}{1+x}tan\left(\frac{\frac{\pi}{2}x}{1+x}\right) \quad (15)$$

$$\frac{k^2 31}{1+k^2 31}=\frac{\pi}{2}(1+x)tan\left(\frac{\pi}{2}x\right) \quad (16)$$

Another parameter called effective coupling coefficient of an arbitrary resonator (k_{eff}) is given as-

$$\frac{k^2 eff}{1+k^2 eff}=\frac{F^2 a-F^2 r}{F^2 r} \quad (19)$$

Piezoelectric charge coefficient(d) is the ratio between electric charge generated per unit Applied Stress expressed in C/N

$$d=\frac{charge\ density\ (open\ circuit)}{Applied\ stress} \quad (20)$$

$$d=k\sqrt{\varepsilon o\ k^T\ s^E} \quad (21)$$

Here s is the compliance (10^{-12} m^2/N), rest of the notations have been discussed above

Piezoelectric Voltage Coefficient(g) is the ratio of electric field produced over mechanical stress applied expressed as Vm/N

$$g=\frac{d}{\varepsilon} \quad (22)$$

d is the charge density and $\varepsilon$is the relative permittivity

$$s=\frac{1}{Y} \quad (23)$$

$$s=\frac{strain}{stress} \quad (24)$$

$$s=\frac{l^2}{\rho v^{\square^2} N} \quad (25)$$

Here Y is the Young's Modulus of elasticity and l is the length $\rho$is the density and v is the sonic velocity($v=2\pi fl$)

$$stress = \frac{Mechanical\ Force\ Applied}{Area} \quad (26)$$

$$strain = \frac{change\ in\ length\ of\ the\ material}{initial\ length} \quad (27)$$

$$g = \frac{Field\ Developed}{Applied\ Mechanical\ Stress} \quad (28)$$

The figure(4) below shows the electrical schematic of the piezoelectric generator

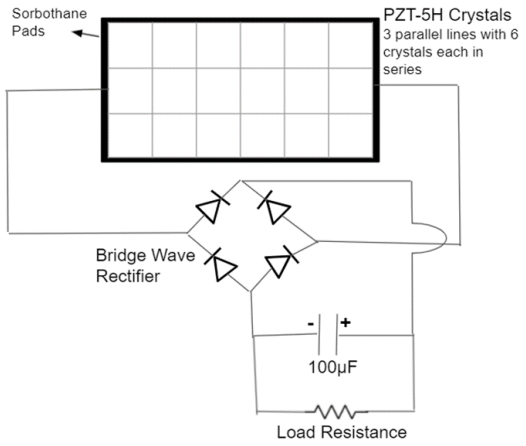

Figure-4: Electrical Schematic of Piezoelectric Generator

A total of 18 small PZT crystals are used with 6 placed in series in order to increase the generated voltage and 3 such parallel lines are used in order to maximise the output current as the total current would be the sum of the current generated by all the individual lines. Next is a full wave bridge rectifier so that the current flows in a single direction only. The output of the rectifier is fed to the capacitor. This capacitor stores the charge and supplies it to the load resistance as per it is needed. The PZT crystals are kept in their place firmly by sorbothane pads, these pads also protect the crystals from any damage. These pads also increase the amount of voltage generated marginally as they also produce mechanical stress on the PZT crystals.

Assuming the ocean/sea current speed to be 1.7778m/s [32] and if water molecules come to rest after colliding with the PZT layer. We are using crystals of dimensions 8cms length, 6cms width and 3cms height. Since there are 18 such crystals, the total area of the cross section would be 864 cm^2. Assuming water molecules at a depth of 5 metres can reach and collide with the PZT crystals and density of seawater is 1023.6kg/m^3. So the stress generated by water molecules on the PZT crystals would be approximately 3233.24265 N/m^2. Stress on each crystal is 179.624591667 N/m^2.

Now voltage generated by each crystal can be found out using equation(22) ,putting the values(g for PZT is 0.025Vm/N) it comes out to be 0.269436Volts. Since there are 6 such crystals in series therefore total voltage generated 1.617 Volts.

CONCLUSION

The study involves the centrifugation of cane juice. The juice is subjected to centrifugation directly after milling of the cane. This treatment has been thought of particularly to clarify juices by removing the suspended particles, viz. silica, organic salts, etc. along with mud. In this paper the design pattern of the centrifuge has been shown. The effective factors such as removal of suspended particles, clarity and ICUMSA colour of the centrifuged juice has shown by the table and graph.

REFERENCES

[1] Curie Temperature Anomaly in Lead Zirconate Titanate/Silver Composites Hae Jin Hwang,*,† Toru Nagai,*,‡ Tatsuki Ohji,*,† Mutsuo Sando,† and Motohiro Toriyama† National Industrial Research Institute of Nagoya, Nagoya 462–8510, Japan Fine Ceramics Research Association, Nagoya 462–8510, Japan Koichi Niihara* The Institute of Scientific and Industrial Research, Osaka University, 8-1 Mihogaoka, Ibaraki, Osaka 567, Japan

[2] International Journal of Advanced Research in Engineering and Technology (IJARET) Volume 12, Issue 3, March 2021, pp. 182-195, Article ID: IJARET_12_03_020 Available online at http://www.iaeme.com/IJARET/issues.asp?JTyp

e=IJARET&VType=12&IType=3 ISSN Print: 0976-6480 and ISSN Online: 0976-6499 DOI: 10.34218/IJARET.12.3.2021.020 "AN INVESTIGATION AND IMPLEMENTATION OF SOLAR-THERMAL BASED HYBRID ENERGY HARVESTING SYSTEM FOR WSN"

[3] Wang, J.; Sandu, C. S.; Colla, E.; Wang, Y.; Ma, W.; Gysel, R.; Trodahl, H. J.; Setter, N.; Kuball, M. (2007-03-26). "Ferroelectric domains and piezoelectricity in monocrystalline Pb(Zr,Ti)O3 nanowires". Applied Physics Letters. 90 (13): 133107. Bibcode:2007ApPhL..90m3107W. doi:10.1063/1.2716842. ISSN 0003-6951. S2CID 123121473.

[4] Wang, Zhaoyu; Hu, Jie; Suryavanshi, Abhijit P.; Yum, Kyungsuk; Yu, Min-Feng (October 2007). "Voltage Generation from Individual BaTiO3Nanowires under Periodic Tensile Mechanical Load". Nano Letters. 7 (10): 2966–2969. Bibcode:2007NanoL...7.2966W. doi:10.1021/nl070814e. ISSN 1530-6984. PMID 17894515

[5] Liu, Huicong; Zhong, Junwen; Lee, Chengkuo; Lee, Seung-Wuk; Lin, Liwei (December 2018). "A comprehensive review on piezoelectric energy harvesting technology: Materials, mechanisms, and applications". Applied Physics Reviews. 5 (4) 041306. Bibcode:2018ApPRv...5d1306L. doi:10.1063/1.5074184. ISSN 1931-9401.

[6] Hutson, Andrew R. "Piezoelectric devices utilizing aluminum nitride." U.S. Patent 3,090,876, issued May 21, 1963. Cook, W. R.; Berlincourt, D. A.; Scholz, F. J. (May 1963). "Thermal Expansion and Pyroelectricity in Lead Titanate Zirconate and Barium Titanate". Journal of Applied Physics. 34 (5): 1392–1398. Bibcode:1963JAP....34.1392C. doi:10.1063/1.1729587. ISSN 0021-8979.

[7] Warner, A. W.; Onoe, M.; Coquin, G. A. (December 1967). "Determination of Elastic and Piezoelectric Constants for Crystals in Class (3m)". The Journal of the Acoustical Society of America. 42 (6): 1223–1231. Bibcode:1967ASAJ...42.1223W. doi:10.1121/1.1910709. ISSN 0001-4966.

[8] Kenisarin, M; Mahkamov, K (2007). "Solar energy storage using phase change materials". Renewable and Sustainable –1965. 11 (9): 1913–1965. doi:10.1016/j.rser.2006.05.005.

[9] Sharma, Atul; Tyagi, V.V.; Chen, C.R.; Buddhi, D. (2009). "Review on thermal energy storage with phase change materials and applications". Renewable and Sustainable Energy Reviews. 13 (2): 318–345. doi:10.1016/j.rser.2007.10.005.

[10] "ENRG Blanket powered by BioPCM". Phase Change Energy Solutions. Retrieved March 12, 2018.

[11] "Heat storage systems" (PDF) by Mary Anne White, brings a list of advantages and disadvantages of Paraffin heat storage. A more complete list can be found in AccessScience website from McGraw-Hill, DOI 10.1036/1097-8542.YB020415, last modified: March 25, 2002 based on 'Latent heat storage in concrete II, Solar Energy Materials, Hawes DW, Banu D, Feldman D, 1990, 21, pp.61–80.

[12] Wave and Ocean Thermal Energy Devices source: http://www.alternative-energy-tutorials.com/wave-energy/wave-energy-devices.html https://energy.gov/eere/energybasics/articles/ocean-thermal-energy-conversion-basics http://www.seao2.com/otec/

[13] Estimation of solar radiation and optimum tilt angles for south-facing surfaces in Humid Subtropical Climatic Region of India - Scientific Figure on ResearchGate. Available from: https://www.researchgate.net/figure/Comparison-of-average-maximum-total-solar-radiation-for-Aligarh-and-New-Delhi_fig4_309345713 [accessed 1 Jul, 2021]

[14] Analyzing lifetime of energy harvesting underwater wireless sensor nodes-H. Emre Erdem | V. Cagri Gungor

[15] A low cost and high efficient acoustic modem for underwater sensor networks A. Sanchez, S.Blanc, P. Yuste , J.J. Serrano Universitat Politècnica de València Cmno. De Vera s/n. Valencia, 46022 SPAIN

[16] Underwater thrust and power generation using flexible piezoelectric composites: an experimental investigation toward self-powered swimmer-sensor platforms Alper Erturk1 and Ghislain Delporte2 1 G W Woodruff School of

Mechanical Engineering, Georgia Institute of Technology, Atlanta, GA 30332-0405, USA 2 Institut Catholique d'Arts et M´etiers, 59800 Lille, France

[17] Underwater sensor networks: applications, advances and challenges BY JOHN HEIDEMANN1,*, MILICA STOJANOVIC2 AND MICHELE ZORZI3

[18] Underwater Sensor Nodes and Networks-Jaime Lloret

[19] Underwater Sensor Network Applications: A Comprehensive Survey Emad Felemban,1 Faisal Karim Shaikh,1,2 UmairMujtaba Qureshi,2 Adil A. Sheikh,1 and Saad Bin Qaisar3

[20] Design of Sensor Nodes In Underwater Sensor Networks- Yu Yang, Zhang Xiaomin, Peng BO, Fu Yujing College Of Marine Northwestern Polytechnical University Xi'an, China

[21] An Energy Harvesting Scheme for Underwater Sensor Applications- Hamid Fahim Rezaei, Anton Kruger, Craig Just

[22] Research Challenges and Applications for Underwater Sensor Networking John Heidemann, Wei Ye, Jack Wills, Affan Syed, Yuan Li Information Sciences Institute, University of Southern California

[23] https://sensortechcanada.com/technical-notes/piezoelectric-fundamentals/

[24] https://www.memsnet.org/material/leadzirconatetitanatepzt/

[25] Beeri, Ofer & Rotem, Oded & Hazan, Eden & Katz, Eugene & Braun, Avi & Gelbstein, Yaniv, "Hybrid photovoltaic-thermoelectric system for concentrated solar energy conversion: Experimental realization and modeling," Journal of Applied Physics, pp: 118, 2015.

[26] Q. Brogan, T. O'Connor, and D. S. Ha, "Solar and thermal energy harvesting with a wearable jacket," IEEE International Symposium on Circuits and Systems (ISCAS), Melbourne VIC, pp. 1412-1415, 2014

[27] A. M. Abdal-Kadhim and K. S. Leong, "Application of thermal energy harvesting from low-level heat sources in powering up WSN node," 2017 2nd International Conference on Frontiers of Sensors Technologies (ICFST), Shenzhen, 2017, pp. 131-135.

[28] G. Verma, V. Sharma, 2019. Analysis of Sb2Te3 and Bi2Te3 materials for enhancing the performance of thermoelectric energy harvester for WSN applications. Recent Patents on Engineering.

[29] L. Hou and S. Tan, "A preliminary study of thermal energy harvesting for industrial wireless sensor networks," 2016 10th International Conference on Sensing Technology (ICST), Nanjing, 2016, pp. 1-5

[30] G. Verma, V. Sharma, "A Novel Thermoelectric energy harvester for Wireless Sensor Network Application", IEEE transaction on Industrial Electronics, Vol 66, Iss 5, Aug 2018, pp: 3530 - 3538.

[31] R. Vlach, "Novel approach to thermoelectric generator modeling as energy harvesting system," Proceedings of the 16th International Conference on Mechatronics - Mechatronika 2014, Brno, 2014, pp. 725-728.

[32] https://oceanservice.noaa.gov/facts/gulfstreamspeed.html#:~:text=The%20velocity%20of%20the%20current,(6.4%20kilometers%20per%20hour).